A Single Nucleotide Linked to a Switch in Metal Ion Reactivity Preference in the HDV Ribozymes†

Anne T. Perrotta and Michael D. Been*

Department of Biochemistry, Box 3711, Duke University Medical Center, Durham, North Carolina 27710

Received December 14, 2006; Revised Manuscript Received March 3, 2007

ABSTRACT: The two ribozymes of hepatitis delta virus (HDV) cleave faster in divalent metal ions than in monovalent cations, and a variety of divalent metal ions can act as catalysts in supporting these higher rates. Although the ribozymes are closely related in sequence and structure, they display a different metal ion preference; the genomic form cleaves moderately faster in Mg^{2+} than in Ca^{2+} while the reverse is true for the antigenomic ribozyme. This difference raises questions about understanding the catalytic role of the metal ion in the reaction. We found that the metal ion reactivity preference correlated with the identity of a single nucleotide 5′ of the cleavage site (−1 position). It is a U in the genomic sequence and a C in the antigenomic sequence. With both ribozymes, the reactivity preference for Mg^{2+} and Ca^{2+} could be reversed with a change at this position (C to U or U to C). Moreover, with an A at position −1, there was a relative increase in cleavage rates in low concentrations of Mn^{2+} for both ribozymes. Metal ion reactivity preference was also linked to changes in pH, and the pH−rate profiles could be shifted with nucleotide changes at position −1. Together, the data provide biochemical evidence in support of an organized active site, as seen in the crystal structures, where at least one metal ion, an ionizable group, and the conformation of the phosphate backbone at the cleavage site interact in concert to promote cleavage.

The ribozymes found in the genomic and antigenomic RNAs of hepatitis delta virus (HDV)[1] are self-cleaving RNAs that generate a 5′-OH group and a 2′,3′-cyclic phosphate group upon cleavage (*1*, *2*). The HDV self-cleaving ribozymes catalyze this reaction in high concentrations of monovalent salts (e.g., 0.5−4 M LiCl); however, much higher rates of cleavage are seen in physiological concentrations of divalent metal ions (e.g., 1−2 mM Mg^{2+} or Ca^{2+}) (*3*−*7*). Although the ribozyme structure is mostly defined by the sequence 3′ of the cleavage site, crystal structures of the HDV genomic ribozyme reveal a metal bound in the active site of the ribozyme precursor (*8*) that is not observed in the ribozyme 3′ product (*9*). This finding suggests that the precursor contributed ligands for the metal which are not present in the 3′ fragment by itself. Indeed, in the precursor structures, the metal ion can form outer sphere contacts to backbone phosphate oxygens not present in the 3′ cleavage product (*8*).

Metal ions associated with RNA can serve both catalytic and structural roles that could be required for ribozyme activity (*10*, *11*). For the HDV ribozymes, structural and biochemical evidence would be consistent with a model in which at least one metal ion positioned in the active site prior to cleavage could be acting as a catalytic cofactor (*6*, *8*). We had also found that changing the phosphodiester bond at the substrate cleavage site from a 3′,5′ to 2′,5′ linkage affected relative rates in different metal ions (*12*). More recently, an analysis of the Mg^{2+} concentration and pH dependence of the HDV genomic ribozyme reaction revealed a relationship that was consistent with a model in which binding of either one or two divalent metal ions supports cleavage activity (*5*, *6*). Furthermore, it was suggested that one of the bound metal ions could have a direct catalytic role and function as a general acid−base catalyst to facilitate proton transfer from the attacking 2′-OH group. However, in the crystal structure it is difficult to reconcile the position of the only observed active site divalent metal ion with a role for it as a proton acceptor to activate the 2′-OH group of nucleotide −1 (*8*).

If a metal ion is directly involved in catalyzing a rate-determining step, both ribozyme reactions might be predicted to show a consistent preference in metal ion reactivity that is related to the properties of the metal ions (charge, size, hardness, coordination geometry, pK_a of bound water, etc.). However, we have observed that the HDV antigenomic ribozyme cleaved slightly faster in Ca^{2+} than in Mg^{2+}, while the genomic ribozyme cleaved faster in Mg^{2+}. This difference seemed incompatible with, for example, a rate-determining step in which the metal ion acted a general acid−base catalyst because the rates might then be expected to show a more consistent dependence on the pK_a of the hydrated metal ion.

The two HDV ribozymes can adopt very similar overall secondary structures but they are not identical in sequence. A seemingly minor difference in sequence is that the genomic ribozyme has a uridine 5′ to the cleavage site (−1 position) whereas the antigenomic ribozyme has a cytidine at position −1. Here we show that changing the U to C or the C to U at position −1 reversed the Mg^{2+}/Ca^{2+} preference in both

† Supported by National Institutes of Health Grant GM047233.

* To whom correspondence should be addressed. E-mail: been@biochem.duke.edu. Telephone: (919) 684-2858. Fax: (919) 684-5040.

[1] Abbreviations: HDV, hepatitis delta virus; nt, nucleotide; EDTA, (ethyelenedinitrilo)tetraacetic acid; Tris, tris(hydroxymethyl)aminomethane; MES, 2-(*N*-morpholino)ethanesulfonic acid.

10.1021/bi602569x CCC: $37.00
Published on Web 04/07/2007

the genomic and antigenomic ribozyme cleavage reactions. Mutations at position −1 also altered the pH−rate profile of the reaction, and the metal ion reactivity preference order can be sensitive to pH. Together, these data provide evidence that a divalent metal ion which is located close to the cleavage site influences the rate of ribozyme cleavage.

MATERIALS AND METHODS

Ribozymes and General Methods. Construction of the plasmids containing the wild-type ribozyme sequences used here has been described (*13*−*15*). For the −1 variants, sequence changes were introduced into the plasmids using oligonucleotide-directed mutagenesis (*16*, *17*). Precursor RNA was prepared by in vitro transcription with T7 polymerase (*18*) from linearized plasmid DNA. The RNA was radiolabeled by including [α-^{32}P]CTP or [α-^{32}P]ATP in the transcription reactions, and the precursor RNA was purified by gel electrophoresis. The isolated RNA was stored frozen at −20 °C in 0.1 mM EDTA. T7 polymerase was prepared by M. Puttaraju; all other enzymes, the nucleotides, and reagents are from commercial suppliers.

Ribozyme Cleavage Kinetics. Prior to the cleavage reactions, the ribozyme precursor was heat denatured at 95 °C for 3 min in 10 mM Tris-HCl, pH 7.5, and 0.1 mM EDTA and then renatured with the addition of 0.1 mM spermidine at 37 °C for 10 min. The RNA was diluted into 50 mM buffer at the desired pH, and the reaction shifted to 25 °C for at least 5 min before initiating the reaction with the addition of metal ion. For the reactions at pH 7.5 where the metal ion concentrations were varied, the buffer was Tris-HCl. For the pH−rate curves, two three-buffer systems were used: 25 mM acetic acid/25 mM MES [2-(*N*-morpholino)ethanesulfonic acid]/50 mM Tris-HCl (AMT buffer, pH 4.0−8.0) or 50 mM MES/25 mM Tris-HCl/25 mM AMP (2-amino-2-methyl-1-propanol) (MTA buffer, pH 7.0−10.0) (*19*). MTA buffer was also used in the metal ion experiments at pH 8.7. Aliquots for each time point were terminated with 2 volumes of formamide/running dyes containing 0.1 M EDTA. For reactions containing higher metal ion concentrations, the reactions were first terminated with excess 0.5 M EDTA, and then the formamide/dye mix was added. The RNA products were separated by polyacrylamide−urea gel electrophoresis, and the fraction cleaved at each time was quantified using a PhosphorImager and ImageQuant software.

Most of the kinetic data were collected manually, in which case the earliest time points were at 3−4 s. In comparisons to data collected with a rapid quench apparatus we found this approach allowed an estimate for rate constants up to about 40−60 min^{-1} (see Figure 3a below), assuming the reactions followed a first-order reaction. A burst or lag in the first few seconds would go undetected with data collected manually; however, we have not seen evidence for a biphasic kinetics in these reactions where data were collected on a rapid quench apparatus (data not shown). At a minimum, rate constants in excess of 20 min^{-1} obtained from data collected by hand provided reasonable estimates that allow a qualitative comparison of relative rates. The metal ion concentration in all reactions greatly exceeded the concentration of the labeled RNA. For each cleavage reaction the rate constant k_{obs} for self-cleavage is obtained by fitting the fraction cleaved (f) at time (t) to the first-order rate equation

Scheme 1

$$R + nM \xleftrightarrow{K_{d,app}} R \bullet M_n \xrightarrow{k_c} P$$

Scheme 2

$$\begin{array}{ccccc} R + M1 & \xleftrightarrow{K_{d1}} & R_{M1} + M2 & \xleftrightarrow{K_{d2}} & R_{M1}^{M2} \\ & & \downarrow k_1 & & \downarrow k_2 \\ & & P & & P \end{array}$$

$f = F(1 - e^{-k_{obs}(t)})$, where F is the end point for the reaction (KaleidaGraph; Synergy Software).

Metal Ion Concentration Rate Curves. k_{obs} for each reaction was plotted against the total metal ion concentration minus the concentration of EDTA in the reaction. The curves shown in the figures were generated by fitting the rate data to either of two models. Scheme 1: n metal ion binding sites in the ribozyme (R) bind n metal ions to generate the active ribozyme·metal ion complex, R·M$_n$, that cleaves, with rate constant k_c, to generate products.

$$k_{obs} = k_c \frac{[R \cdot M_n]}{[R]_{total}} = k_c \frac{[M]^n}{[Me]^n + K_{d,app}} \quad (1)$$

Much of the kinetic data for the antigenomic ribozyme and variants (at pH 7.5) can be fit using eq 1, and the value for n (the Hill value) varies from ∼0.5 to 2.0 (data not shown). This suggested that there may be at least two classes of metal-binding site, but the cooperativity of the binding varies with the −1 mutation, the metal ion, and pH of the reaction.

Scheme 1 does not describe the behavior of ribozyme metal ion combinations in which the rate−metal ion curves are bell-shaped. The shape of these curves suggest that metal ions bind to at least two classes of metal sites, and the ribozyme was active with either one or two metal ions bound. Moreover, the two metal ion ribozyme complexes cleave with different rates (Scheme 2), and this difference can be most apparent when k_2 is less than k_1.

$$k_{obs} = k_1 \frac{[R_{M1}]}{[R]_{total}} + k_2 \frac{[R_{M1}^{M2}]}{[R]_{total}} = \frac{k_1[Me]K_{d2} + k_2[Me]^2}{K_{d1}K_{d2} + K_{d2}[Me] + [Me]^2} \quad (2)$$

Scheme 2 makes assumptions about the number of sites, their relationship, order of binding, etc., that may not be justified. However, eq 2, derived from this scheme, generates curves that aid visually in presenting the data in the metal concentration−rate curves. Although the values obtained in the curve fitting for dissociation and rate constants appeared reasonable, the introduction of the fourth variable often resulted in large errors. For that reason, and especially because we have not established the correctness of the model, we did not report the kinetic values determined with this curve fitting.

RESULTS

Description of the Precursor RNAs. The RNA sequences used for HDV genomic and antigenomic ribozymes in this study were similar in size. The antigenomic form (PEX1) (Figure 1a) had 8 nt 5′ to the cleavage site and 93 nt 3′ of the cleavage site. The genomic (TGR1) (Figure 1b) had 4 nt 5′ to the cleavage site and 85 nt 3′ of the cleavage site.

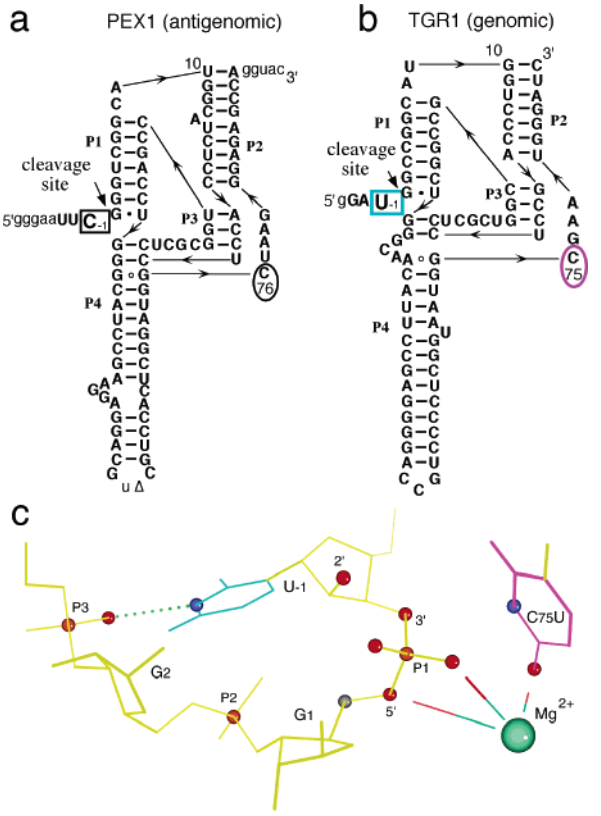

FIGURE 1: The HDV ribozymes. (a, b) Sequence and secondary structures of the antigenomic ribozyme (PEX1) and the genomic ribozyme (TGR1) precursors. The −1 nucleotide position is boxed, and an oval is drawn around the catalytic cytosine. Lower case letters represent the non-wild-type sequence. The sequence of hairpin loop 4 in PEX1 differs from several clinical isolates by a nucleotide deletion (△). (c) Illustration of the bend in the backbone at the cleavage site phosphate in the genomic C75U ribozyme precursor in Mg^{2+} (PDB code 1SJ3), solved by Ke et al. (*8*). Only a subset of the atoms close to the Mg^{2+} are shown; the distances from the metal ion to O4 of U75 and the nonbridging and 5′ bridging oxygen on the scissile phosphate are 2.2, 3.7, and 4.3 Å, respectively. The distance from the metal ion to the center of the pyrimidine ring at −1 is about 10 Å. This figure was prepared with Mage software (*31*).

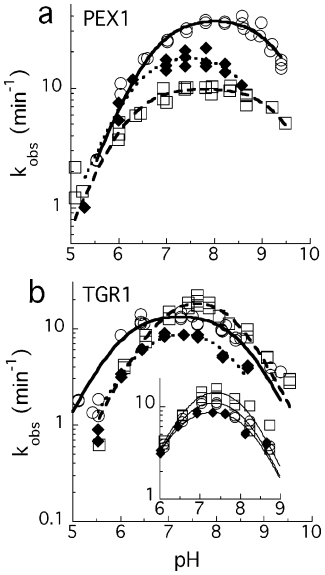

FIGURE 2: pH−rate curves for the wild-type precursors in divalent cations. (a) Rate of cleavage for the antigenomic sequence as a function of pH in 10 mM Ca^{2+} (circles), Mg^{2+} (squares), or Mn^{2+} (closed diamonds). (b) pH−rate profiles for the genomic sequence in 10 mM divalent cations [symbols as in (a)]. (b, inset) rate−pH profiles for the genomic sequence in 1 mM divalent cations. All reactions were at 25 °C. The curves were generated by fitting the pH−rate data to the equation $k_{obs} = k_c/(1 + 10^{pK_{a1}-pH} + 10^{pH-pK_{a2}} + 10^{pK_{a1}-pK_{a2}})$.

The core of both PEX1 and TGR1 were the wild-type sequence. For the cleavage site variants used here, single-base changes were introduced at the −1 position (5′ to the cleavage site); otherwise, each of the variant ribozymes is identical to the starting sequence. The ribozymes cleaved with first-order kinetics giving end points of 70−90% cleavage, depending on the ribozyme and the reaction conditions. To facilitate manual collection of the time points in the kinetic studies, the temperature of the reactions was 25 °C rather than 37 °C. Nevertheless, with some constructs, rate constants in excess of 20 min^{-1} were observed under favorable pH and metal ion concentrations. A comparison of rates measured by hand and with a rapid quench instrument indicated that, for comparison of relative rates, rate constants obtained manually were adequate for all but the fastest reactions.

The Genomic and Antigenomic Ribozymes Differed in Metal Ion Preference. pH−rate curves were generated for cleavage of the antigenomic (PEX1) ribozyme reaction in 10 mM Mg^{2+}, Ca^{2+}, or Mn^{2+} (Figure 2a). In the optimal pH range of 7−8, the highest rates were in Ca^{2+}. In contrast, with the genomic ribozyme (TGR1) (Figure 2b), the higher rates were in Mg^{2+}. However, a shift in the pH−rate curves for the genomic ribozyme also revealed that, below pH 7, cleavage rates in Ca^{2+} could exceed those in Mg^{2+}. This pH-dependent change in metal ion preference was only seen with the high metal ion concentrations (10 mM) used in these reactions (see below). In lower metal ion concentrations (1 mM) (Figure 2b inset) the pH−rate curves with the genomic ribozyme were nested, with the highest rates in Mg^{2+} and slowest in Mn^{2+}.

Cleavage rate constants of antigenomic and genomic ribozymes in increasing concentrations of different metal ions, Mg^{2+}, Ca^{2+}, and Mn^{2+}, were compared at pH 7.5 (Figures 3a and 4a). The rates for both ribozymes increased with concentrations of Mg^{2+} or Ca^{2+}. However, there were differences in the profiles of the metal ion concentration−rate curves for the two ribozymes. With the antigenomic ribozyme, high concentrations of metal ion (∼50−100 mM) were required (Figure 3a) to approach a maximum rate, and the Mg^{2+} or Ca^{2+} concentration giving half-maximal rates ($K_{1/2}$) was 10 mM or greater. The cleavage rates with the genomic ribozyme (TGR1) showed saturation at much lower concentrations of both Mg^{2+} and Ca^{2+} (Figure 4a), with maximal rates at about 10 mM and a $K_{1/2}$ of about 1 mM. In general, over a range of concentrations, the antigenomic ribozyme cleaved about 2-fold faster in Ca^{2+} than in Mg^{2+}, whereas the genomic ribozyme cleaved about 2-fold faster in Mg^{2+} than in Ca^{2+}. This relative difference was mainly due to the difference in the rates in Ca^{2+} because both ribozymes cleaved at roughly similar rates (∼20 min^{-1}) in high concentrations of Mg^{2+} (10−100 mM).

There was evidence of bell-shaped metal ion concentration curves indicating a second class of metal-binding sites. At low metal ion concentration (∼0.1 mM), the genomic ribozyme showed highest activity in Mn^{2+}, but those rates decreased when the Mn^{2+} concentration exceeded 1 mM

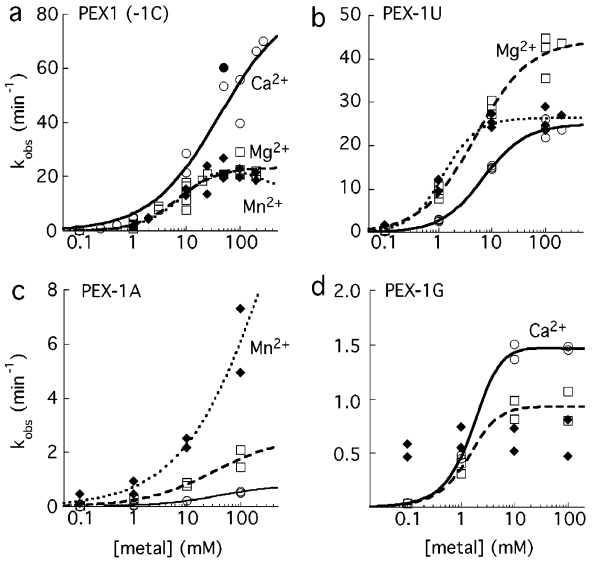

FIGURE 3: Metal ion concentration−rate curves for PEX1 and −1 variants. All reactions were done at pH 7.5 and 25 °C. (a) Rate of cleavage for the PEX1 (wt) antigenomic sequence as a function of [metal ion] in Ca^{2+} (circles), Mg^{2+} (squares), or Mn^{2+} (closed diamonds). The closed circle and closed square at 50 mM Ca^{2+} and Mg^{2+} were rate constants determined from data collected using the rapid quench apparatus. All other data were collected manually. (b−d) Variants PEX-1U, PEX-1A, and PEX-1G, respectively. Symbols are the same as for (a). The data for PEX-1G in Mn^{2+} (d) could not be reasonably fit with either eq 1 or 2, so no curve is shown.

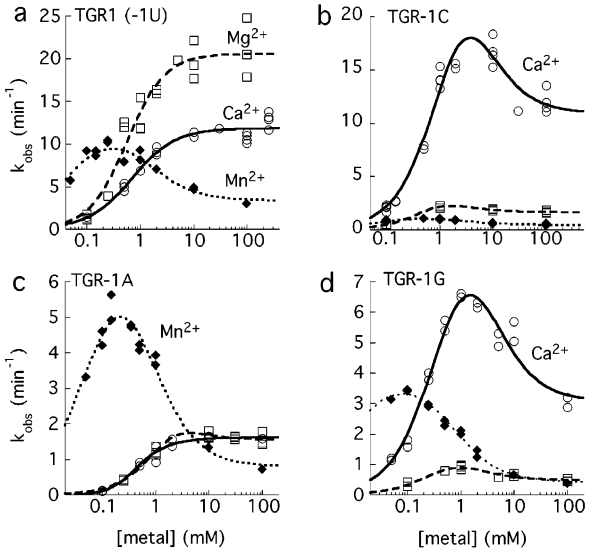

FIGURE 4: Metal ion concentration−rate curves for TGR1 and −1 variants. All reactions were done at pH 7.5 and 25 °C, and the symbols are the same as for Figure 3. (a) TGR1 (wt) genomic sequence. (b−d) Variants TGR-1C, TGR-1A, and TGR-1G, respectively.

(Figure 4a). Bell-shaped concentration curves in Ca^{2+} and Mg^{2+} were also seen with some of the −1 variants (see below), suggesting that this bell shape is not just a Mn^{2+} artifact.

Altering the Nucleobase at the −1 Position Changed the Metal Ion Reactivity Preference. Whereas the genomic ribozyme has a U at position −1, the antigenomic ribozyme has a C at that position (Figure 1). The possibility that a metal ion preference could be related to the identity of the nucleobase at this position was tested after making base changes at position −1. Changing −1C to U in the antigenomic ribozyme (PEX-1U) caused the rate of cleavage to decrease in Ca^{2+} and to increase in Mg^{2+} (Figure 3b). The −1U to C change in the genomic ribozyme (TGR-1C) resulted in a 10-fold decrease in activity in Mg^{2+} and a small (∼1.5-fold) increase in Ca^{2+} (Figure 4b). As a result, the TGR-1C has a relative metal ion preference similar to wild-type PEX1 (−1C) (Figure 3a), and PEX-1U has a relative preference similar to wild-type TGR1 (−1U) (Figure 4a). Thus, there appeared to be a linkage between the nucleobase at position −1 and cleavage rates in Mg^{2+} and Ca^{2+}.

With G or A at the −1 position, both ribozymes cleaved slower, but again, there was a change of the metal ion preference with the nucleobase at −1. PEX-1A (Figure 3c) cleaved fastest in Mn^{2+}, while in Ca^{2+} it was 100-fold slower than the wild type. With TGR-1A (Figure 4c), cleavage rates in low metal ion concentrations were also fastest in Mn^{2+}, although the bell-shaped response resulted in relatively higher rates in Ca^{2+} or Mg^{2+} as the concentrations increased (above ∼10 mM). The −1G variants, PEX-1G and TGR-1G, cleave fastest in Mn^{2+} at very low concentrations of metal ion, but at higher concentrations, the fastest rates were in Ca^{2+} (Figures 3d and 4d). The bell-shaped response to metal ion concentrations (Mg^{2+}, Ca^{2+}, and Mn^{2+}) was especially apparent in the TGR-1G reactions.

The highest rates of ribozyme cleavage show a consistent correlation between the −1 nucleobase and an order of reactivity preference for metal ion at pH 7.5. These data suggest that at least one metal ion binding site is partially specified either by the −1 nucleotide or by a region of the ribozyme in close proximity to that nucleotide, and occupancy of this site by a metal ion contributes to (or affects) the observed cleavage rate.

Metal Ion Concentration−Rate Curves Suggested Two Classes of Metal Ion Binding Sites. As already noted, metal ion rate curves were bell-shaped for certain ribozyme and metal ion combinations. This bell-shaped response was very apparent with the genomic ribozyme and its −1 variants in increasing concentrations of Mn^{2+}. A combined plot of the Mn^{2+} data at pH 7.5 for the −1 variants shows that the metal ion concentration dependence does vary with the −1 nucleobase (Figure 5a). However, bell-shaped curves were also evident in Ca^{2+} for TGR-1G (Figure 4d) and in other metal ion−ribozyme combinations if the pH of the reaction was increased (data not shown; see below). The antigenomic ribozymes showed less evidence for a decrease in cleavage rate with higher metal ion concentrations under the standard conditions we used, but the PEX1−metal concentration curve became bell-shaped when the reaction pH was increased. At pH 8.7, the response of PEX1 to increasing Mn^{2+} concentrations was also bell-shaped (Figure 6). We consider it unlikely that the bell-shaped response of PEX1 in Mn^{2+} could be due to nonspecific effects such as aggregation at the higher pH and metal ion concentrations because the peak activity with the genomic ribozymes (Figures 4 and 5a) occurred at much lower concentrations, closer to 1 mM Mn^{2+}, and at pH 7.5. A nonspecific interaction of the metal ion and RNA that slowed the reaction should result in inhibition of both ribozymes at similar metal ion concentrations.

The pH−Rate Curve Is Sensitive to the Nucleobase at Position −1. In 1 mM Mn^{2+}, the pH−rate curve of the genomic HDV ribozyme was bell-shaped, relatively narrow,

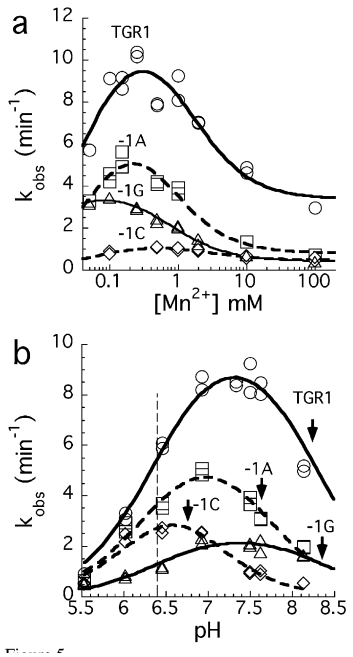

FIGURE 5: Bell-shaped metal ion concentration−rate and pH−rate curves for cleavage of the genomic ribozyme and variants in Mn^{2+}. (a) The Mn^{2+} cleavage data (at pH 7.5) for TRG1 (circles) and the three −1 variants (−1A, squares; −1G, triangles; and −1C, diamonds) were plotted on a single graph. (b) pH−rate curves in 1 mM Mn^{2+}. The symbols are the same as in (a). The data were fit to the equation given in the legend to Figure 2; the heavy dashed vertical line is the average apparent pK_a on the ascending slope, and the arrows indicate the second apparent pK_a (see text).

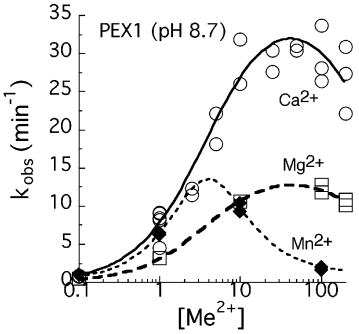

FIGURE 6: Bell-shaped metal ion curves for the antigenomic ribozyme with increased pH. The reactions with PEX1 in three different metal ions were similar to those in Figure 3 but with the pH raised to 8.7.

and with a pH optimum of 7.3 ± 0.2 (Figure 5b). With changes at position −1, particularly U-1A and U-1C, there was a shift in the curve. From the curve fitting, the calculated apparent pK_a values on the ascending side of the curve were nearly the same for all constructs: 6.4 ± 0.1 for TGR1 and the −1C and −1G variants (vertical dashed line, Figure 5b) and 6.3 ± 0.1 for the −1A variant. From previous studies (*3*, *20*−*22*), we assume that this value would correspond to the ionization constant of a proposed catalytic group, C75, common to the ribozyme constructs. The second apparent pK_a (arrows, Figure 5b) varied and was calculated as 8.2 ± 0.1 for TGR1 (−1U), 8.4 ± 0.1 for −1G, 7.6 ± 0.1 for −1A, and 6.8 ± 0.4 for −1C. These values do not correlate with the unperturbed pK_a values for the nucleobase (*23*) at −1, suggesting that ionization of that nucleobase was not immediately responsible for the apparent pK_a observed in these reactions. However, it was this second apparent pK_a that changed with the nucleobase at position −1 and accounted for the shift in the shape of the pH−rate profiles.

DISCUSSION

In this study, we examined the effect that changing the nucleotide 5′ to the cleavage site had on metal ion reactivity preference in the genomic and antigenomic HDV ribozymes. A single nucleotide (or even an abasic ribose) 5′ to the cleavage site is sufficient for cleavage activity in both cis and trans-acting forms of the ribozymes (*16*, *24*−*26*). The two structurally related HDV ribozymes have similar sequence but differ in the nucleotide at the −1 position. In sequences of clinical isolates (*4*), the nucleotide 5′ to the cleavage site in the antigenomic ribozyme was always a C, while in the genomic sequence it was always a U. In the crystal structure of the genomic ribozyme precursor with a C75U mutation (*8*) there is a sharp kink in the backbone at the cleavage site (Figure 1c). In this structure, likely to approximate a ground state structure, the uracil at −1 is positioned such that it could hydrogen bond to a nonbridging phosphate oxygen between nucleotides 2 and 3 (*8*). Before cleavage can occur, the −1 nucleotide is proposed to rotate out of that position so that its 2′-OH group is positioned in-line with the phosphorus and the 5′-O leaving group. Nucleobase changes at −1 are likely to alter a ground state structure, and a particular nucleobase change could either facilitate or limit motion required to approach the transition state structure. We can hypothesize that mutations at the −1 position will affect the position of the 2′-oxygen at nucleotide −1 (the nucleophilic group), the scissile phosphate group, and even the 5′-oxygen at position +1 (the leaving group). If the catalytic metal ion was interacting at any of these positions, perturbing the structure or local environment could alter metal ion preference.

In examining the effect of the −1 position on metal ion preference, we found that the −1 nucleotide−metal ion effect was sensitive to pH and also that binding of a second metal ion could limit cleavage rates. We could not explore all of the possible variations of these parameters (−1 nucleotide, pH, metal ion, and metal ion concentration), so many aspects of this analysis and interpretation are more qualitative than quantitative. With both ribozymes, we found a strong qualitative correlation between the metal ion that supports the highest rate of cleavage and the nucleobase at the −1 position (at pH 7.5). With a U at position −1 the highest rates were in Mg^{2+}, with a C or G the highest rates were in Ca^{2+}, and with an A the highest rates were in Mn^{2+}. Although the differences in rates are not overly large, a change in the metal ion reactivity preference for cleavage was easily detectable. We found it noteworthy that the recently discovered CPEB3 ribozyme in mammals, which is a naturally occurring but slow-cleaving HDV-like ribozyme, has an A at position −1, and it also cleaved fastest in Mn^{2+} (*27*). Our data predict that changing nucleotide −1 to C or U in the CPEB3 ribozyme should enhance its cleavage rate in Ca^{2+} and Mg^{2+}.

We propose that the identity of the nucleobase at position −1 affects metal ion preference by shifting the position of metal ion ligand groups and altering the ionic environment near the cleavage site, but either effect could be indirect with

respect to the nucleobase. The possibility that an absolutely essential catalytic metal binds directly to the nucleobase at position −1 appears to be low because an oligonucleotide with an abasic residue at position −1 is a substrate for cleavage (*26*). Likewise, in the crystal structures, the divalent metal ion that was in the active site was not associated with the nucleobase at position −1 (*8*), although it may recruited in the transition state. Metal ion rescue of a HDV ribozyme that has a thiophosphate substitution at the scissile phosphate was inconclusive in demonstrating metal ion coordination to a nonbridging oxygen. In those experiments, the *pro-*R_P-(*S*) substitution inhibited activity in Mg^{2+}, but it could not be rescued with a softer metal ion (*28*). However, the lack of metal ion rescue is not evidence that a metal ion is not required. An antigenomic HDV ribozyme with a sulfur substitution of the 5′ bridging oxygen has been examined more recently (*29*), and the data demonstrate a requirement for the catalytic cytosine acting as a general acid−base catalyst but not direct coordination of a metal ion at that position. Although there are other interpretations for the data presented in this paper, a linkage between the nucleotide at position −1 and divalent metal ion preference would be consistent with the hypothesis that a metal ion at the active site acts as a cofactor for the reaction.

The bell-shaped metal−concentration curves are unambiguous evidence for at least two metal ion binding sites. A possible model is that cleavage rates first increase as one site becomes occupied, but as the second site is occupied, the rate can be additionally affected (Scheme 2 in Materials and Methods). With binding of the second metal ion, the rate could further increase, level off, or even decrease. The actual shape of the curve may depend on the ribozyme, the nucleobase at position −1, the metal ion, metal ion concentrations, and the pH of the reaction. Bevilacqua and coworkers (*6*) have examined the interplay of pH and metal ion concentrations on the rate of cleavage of a longer version of the genomic ribozyme, and they have evidence of interference with metal ion binding by protonation of a group in the ribozyme. Here, the bell-shaped metal ion curves were most prominent in the genomic ribozyme, so it could be that the bell-shaped curves are related to the interference reported by Nakano et al. (*6*). However, the decrease in activity that we saw was at higher pH and metal ion concentrations, so there is reason to suspect that we could be looking at different metal sites. Our data do suggest that the metal ion preference is due to interactions at a metal site near the −1 nucleotide, rather than at a more distal metal site.

The evidence for two binding sites, one of which may contribute to a slower rate when occupied, does raise the possibility that the basis of the metal ion reactivity preference itself is due to a metal ion limiting or slowing rates rather than enhancing cleavage rates. On the basis of the preferences seen, at least one of the metal ions is binding near the scissile phosphate; while the second may bind at the active site, the data do not rule out the possibility that it binds elsewhere. The data do not distinguish between a metal site that enhances the cleavage rate and a site that limits it. Thus, a model where binding at a site near nucleotide −1 slows cleavage while binding at a distal site enhances cleavage rates could be consistent with the data. A simpler model might be that a catalytic metal binds at the active site at low concentrations but, at higher metal ion concentrations, a second metal can bind there as well. In that case, under the conditions where the bell-shaped curve is seen, the binding of two metal ions interferes with cleavage. A second metal ion in the active site could alter the local structure, perturb the pK_a of an important ionizable group, or affect a conformation change required for cleavage. Ke et al. (*30*) have recently located three monovalent metal ions (Tl^+) bound in the active site region of the genomic ribozyme. Two of the monovalent metal ions occupy the site previously seen to bind a divalent metal ion (*8*), and both Tl^+ ions are competed away with cobalt hexaamine. The third Tl^+ binds at a second site and forms inner sphere contacts with a nonbridging oxygen (corresponding to the *pro-*S_P position for a thiophosphate) on the scissile phosphate and the 2′-oxygen nucleophile. In light of the results presented here, it is tempting to speculate that this site may bind a divalent metal ion; however, that was not observed by Ke et al. (*30*).

The results we present here, especially the metal ion preference changes, underscore the difficulty in correlating physical properties of the metal ions and the rate of the reaction with the HDV ribozymes. For example, demonstrating that the rates of cleavage show a predictable dependence on the pK_a of the hydrated metal ion would support a model in which the metal ion acted as a general acid−base catalyst in the reaction. Nevertheless, the results do support the idea that a metal ion near the cleavage site, though not necessarily the one seen in the crystals (*8*), contributes to enhanced cleavage activity.

ACKNOWLEDGMENT

We thank A. Brown, S. Wilkinson, and S. Crary for comments on versions of the manuscript, I-h. Shih for discussions of models, and A. Ke and J. Doudna for comments and for generously sharing unpublished materials.

REFERENCES

1. Wu, H. N., Lin, Y. J., Lin, F. P., Makino, S., Chang, M. F., and Lai, M. M. (1989) Human hepatitis delta virus RNA subfragments contain an autocleavage activity, *Proc. Natl. Acad. Sci. U.S.A. 86*, 1831−1835.
2. Sharmeen, L., Kuo, M. Y.-P., Dinter-Gottlieb, G., and Taylor, J. (1988) Antigenomic RNA of human hepatitis delta virus can undergo self-cleavage, *J. Virol. 62*, 2674−2679.
3. Nakano, S.-I., Chadalavada, D. M., and Bevilacqua, P. C. (2000) General acid-base catalysis in the mechanism of a hepatitis delta virus ribozyme, *Science 287*, 1493−1497.
4. Wadkins, T. S., and Been, M. D. (2002) Ribozyme activity in the genomic and antigenomic RNA strands of hepatitis delta virus, *Cell. Mol. Life Sci. 59*, 112−125.
5. Nakano, S., Cerrone, A. L., and Bevilacqua, P. C. (2003) Mechanistic characterization of the HDV genomic ribozyme: classifying the catalytic and structural metal ion sites within a multichannel reaction mechanism, *Biochemistry 42*, 2982−2994.
6. Nakano, S.-I., Proctor, D. J., and Bevilacqua, P. C. (2001) Mechanistic characterization of the HDV genomic ribozyme: assessing the catalytic and structural contributions of divalent metal ions within a multi-channel reaction mechanism, *Biochemistry 40*, 12022−12038.
7. Perrotta, A. T., and Been, M. D. (2006) HDV ribozyme activity in monovalent cations, *Biochemistry 45*, 11357−11365.
8. Ke, A., Zhou, K., Ding, F., Cate, J. H., and Doudna, J. A. (2004) A conformational switch controls hepatitis delta virus ribozyme catalysis, *Nature 429*, 201−205.
9. Ferré-D'Amaré, A. R., Zhou, K., and Doudna, J. A. (1998) Crystal structure of a hepatitis delta virus ribozyme, *Nature 395*, 567−574.
10. Pyle, A. M. (2002) Metal ions in the structure and function of RNA, *J. Biol. Inorg. Chem. 7*, 679−690.

11. Sigel, R. K., and Pyle, A. M. (2007) Alternative roles for metal ions in enzyme catalysis and the implications for ribozyme chemistry, *Chem. Rev. 107*, 97−113.
12. Shih, I.-h., and Been, M. D. (1999) Ribozyme cleavage of a 2′,5′-phosphodiester linkage: mechanism and a restricted divalent metal ion requirement, *RNA 5*, 1140−1148.
13. Wadkins, T. S., and Been, M. D. (1997) Core-associated non-duplex sequences distinguishing the genomic and antigenomic self-cleaving RNAs of hepatitis delta virus, *Nucleic Acids Res. 25*, 4085−4092.
14. Wadkins, T. S., Perrotta, A. T., Ferré-D'Amaré, A. R., Doudna, J. A., and Been, M. D. (1999) A nested double-pseudoknot is required for self-cleavage activity of both the genomic and antigenomic HDV ribozymes, *RNA 5*, 720−727.
15. Wadkins, T. S., Shih, I., Perrotta, A. T., and Been, M. D. (2001) A pH-sensitive RNA tertiary interaction affects self-cleavage activity of the HDV ribozymes in the absence of added divalent metal ion, *J. Mol. Biol. 305*, 1045−1055.
16. Perrotta, A. T., and Been, M. D. (1991) A pseudoknot-like structure required for efficient self-cleavage of hepatitis delta virus RNA, *Nature 350*, 434−436.
17. Perrotta, A. T., and Been, M. D. (1992) Cleavage of oligoribonucleotides by a ribozyme derived from the hepatitis δ virus RNA sequence, *Biochemistry 31*, 16−21.
18. Davanloo, P., Rosenberg, A. H., Dunn, J. J., and Studier, F. W. (1984) Cloning and expression of the gene for bacteriophage T7 RNA polymerase, *Proc. Natl. Acad. Sci. U.S.A. 81*, 2035−2039.
19. Perrin, D. D., and Dempsey, B. (1974) *Buffers for pH and Metal Ion Control*, Chapman and Hall, London.
20. Perrotta, A. T., Shih, I.-h., and Been, M. D. (1999) Imidazole rescue of a cytosine mutation in a self-cleaving ribozyme, *Science 286*, 123−126.
21. Shih, I.-h., and Been, M. D. (2001) Involvement of a cytosine side chain in proton transfer in the rate-determining step of ribozyme self-cleavage, *Proc. Natl. Acad. Sci. U.S.A. 98*, 1489−1494.
22. Perrotta, A. T., Wadkins, T. S., and Been, M. D. (2006) Chemical rescue, multiple ionizable groups, and general acid−base catalysis in the HDV genomic ribozyme, *RNA 12*, 1282−1291.
23. Saenger, W. (1984) *Principles of Nucleic Acid Structure*, Springer-Verlag, New York.
24. Perrotta, A. T., and Been, M. D. (1990) The self-cleaving domain from the genomic RNA of hepatitis delta virus: sequence requirements and the effects of denaturant, *Nucleic Acids Res. 18*, 6821−6827.
25. Been, M. D., Perrotta, A. T., and Rosenstein, S. P. (1992) Secondary structure of the self-cleaving RNA of hepatitis delta virus: applications to catalytic RNA design, *Biochemistry 31*, 11843−11852.
26. Shih, I.-h., and Been, M. D. (2001) Energetic contribution of non-essential 5′ sequence to catalysis in a hepatitis delta virus ribozyme, *EMBO J. 20*, 4884−4891.
27. Salehi-Ashtiani, K., Lupták, A., Litovchick, A., and Szostak, J. W. (2006) A genomewide search for ribozymes reveals an HDV-like sequence in the human CPEB3 gene, *Science 313*, 1788−1792.
28. Jeoung, Y.-H., Kumar, P. K. R., Suh, Y.-A., Taira, K., and Nishikawa, S. (1994) Identification of phosphate oxygens that are important for self-cleavage activity of the HDV ribozyme by phosphorothioate substitution interference analysis, *Nucleic Acids Res. 22*, 3722−3727.
29. Das, S. R., and Piccirilli, J. A. (2005) General acid catalysis by the hepatitis delta virus ribozyme, *Nat. Chem. Biol. 1*, 45−52.
30. Ke, A., Ding, F., Batchelor, J. D., and Doudna, J. A. (2007) Structural roles of monovalent cations in the HDV ribozyme, *Structure* (in press).
31. Richardson, D. C., and Richardson, J. S. (1992) The kinemage: A tool for scientific communication, *Protein Sci. 1*, 3−9.

BI602569X